Advances in Concrete Construction, *Vol. 5, No. 3 (2017) 221-240*
DOI: https://doi.org/10.12989/acc.2017.5.3.221

Analysis of quasi-brittle materials at mesoscopic level using homogenization model

Dannilo C Borges[1a] and José J C Pituba[*2]

[1]*Federal University of Goiás, Civil Engineering School, Av. Universitária, 1488, 74605-220, Goiânia, Brazil*
[2]*Federal University of Goiás, Engineering School, Department of Civil Engineering, Laboratory of Computational Modeling, Av. Dr Lamartine Pinto de Avelar, 1120, 75704-020, Catalão, Brazil*

(Received February 26, 2017, Revised May 16, 2017, Accepted May 23, 2017)

Abstract. The modeling of the mechanical behavior of quasi-brittle materials is still a challenge task, mainly in failure processes when fracture and plasticity phenomena become important actors in dissipative processes which occur in materials like concrete, as instance. Many homogenization-based approaches have been proposed to deal with heterogeneous materials in the last years. In this context, a computational homogenization modeling for concrete is presented in this work using the concept of Representative Volume Element (RVE). The material is considered as a three-phase material consisting of interface zone (ITZ), matrix and inclusions-each constituent modeled by an independent constitutive model. The Representative Volume Element (RVE) consists of inclusions idealized as circular shapes symmetrically and non-symmetrically placed into the specimen. The interface zone is modeled by means of cohesive contact finite elements. The inclusion is modeled as linear elastic and matrix region is considered as elastoplastic material. A set of examples is presented in order to show the potentialities and limitations of the proposed modeling. The consideration of the fracture processes in the ITZ is fundamental to capture complex macroscopic characteristics of the material using simple constitutive models at mesoscopic level.

Keywords: concrete; fracture mechanics; finite element; homogenization; plasticity

1. Introduction

The modeling of the mechanical behavior of quasi-brittle materials is still a challenge task, mainly in failure processes when fracture and plasticity phenomena play important roles in dissipative processes which occur in materials like concrete. In fact, as the concrete is a composite material, it presents a very complex mechanical behavior that is very hard to be modeled (see Pituba and Fernandes 2011, Brancherie and Ibrahimbegovic 2009, Zhu *et al.* 2008 and others). Initially, the constitutive phenomenological theories have been represented satisfactorily the mechanical behavior of such materials. As example, the Continuum Damage Mechanics (CDM) provided sophisticated constitutive models to simulate the mechanical behavior of heterogeneous materials, mainly concrete, presenting satisfactory results (see Pituba *et al.* 2016, Pereira Jr *et al.*

*Corresponding author, Professor, E-mail: julio_pituba@ufg.br
[a]Ph.D. Student, E-mail: danniloc@gmail.com

http://www.techno-press.org/?journal=acc&subpage=7 ISSN: 2287-5301 (Print), 2287-531X (Online)

2016, Pituba 2015). Nevertheless, in order to improve the representation of the mechanical behavior of such heterogeneous materials, that kind of constitutive modeling requires a complex formulation as well as a big number of parameters, sometimes hard to identify. However, deformation and rupture processes take place at microscopic level. In this context and taking into account the advances on the computational mechanics, in the last decades many numerical techniques and constitutive models have been proposed to describe the mechanical behavior of heterogeneous materials at microscopic level, Needleman and Tvergaard (1987), Miehe (2003) and Santos and Pituba (2017). Therefore, the structural behavior at macroscopic level is connected to the micromechanical behavior of the material at microscopic level using homogenization techniques leading to a more accurate representation of the macro-continuum behavior, Péric *et al.* (2011) and Miehe and Koch (2002). In this context, some works have been developed to model the mechanical behavior of the concrete (see Gitman 2006, Wriggers and Moftah 2006, and López *et al.* 2008).

One of the main advantages of multi-scale modeling is that the physical phenomena of the concrete can be better evaluated because the mechanical properties of each material of the microstructure and its imperfections and voids can be considered and informations about the microstructure are transferred to the macro-continuum. On the other hand, if the analysis is performed only at macroscopic level using phenomenological constitutive models, the concrete behaves as a continuum material, but its microstructure is composed by several materials presenting different mechanical behaviors.

The phenomena treated by conventional theories, in fact, are a macroscopic reflection of what happens at microstructure. Thus, when analyzing heterogeneous materials, especially the concrete, more efficient constitutive models can be obtained if its microstructure is observed and a multi-scale modeling is considered, where adopting simple constitutive models at the microstructure, complex phenomena can be reproduced at macroscopic level, Pituba and Souza Neto (2015).

In this work only the mechanical behavior of the concrete at mesoscopic level is considered in order to validate qualitatively the proposed modeling. The presented formulation is developed in the context of the multi-scale analysis recently proposed by Fernandes *et al.* (2015a) and Fernandes *et al.* (2015b), where the RVE must be defined as well as homogenization techniques. Also, the Finite Element Method is used on the RVE modeling. In the proposed modeling, the Fracture Mechanics as well as the Plasticity Theory have been considered to model the dissipative phenomena in the interface zone as well as inside the matrix taking into account the geometry and properties of the materials defined at mesoscopic level. The proposed modeling is an alternative to the complex phenomenological constitutive models used to represent the behavior of heterogeneous quasi-brittle materials. Therefore, this work intends to contribute to the knowledge of some complex characteristics of the concrete using a homogenization-based approach at mesoscopic level as well as simple constitutive models. Besides, in future work the proposed modeling will be coupled to a macro-continuum formulation considering damage localization phenomena (Toro *et al*. 2016) in order to perform a full coupled multi-scale analysis.

In what follows, a brief description of the proposed modeling for the concrete is presented in section 2, where the homogenization techniques, the constitutive models based on the Contact and Fracture Mechanics, the Mohr-Coulomb model adopted to represent the matrix behavior, as well as a cohesive contact finite element used to model the interface zone have been discussed. In section 3, numerical examples are analyzed to show the potentialities and limitations of the proposed modeling. Finally, in section 4, final considerations have been discussed.

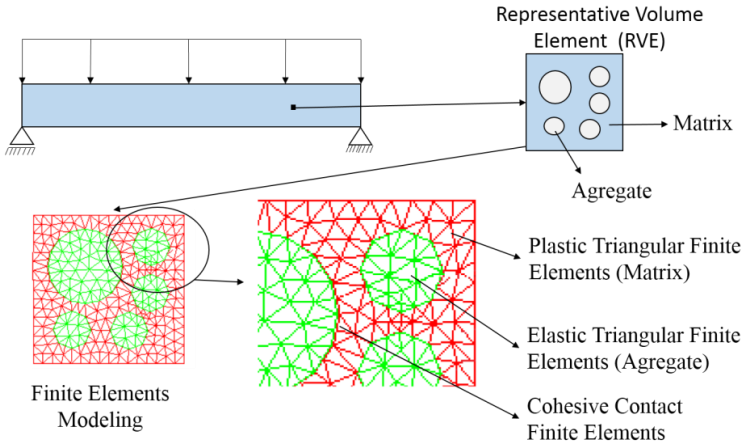

Fig. 1 Multi-scale analysis scheme

2. Multi-scale model for the concrete

This section intends to present the homogenization-based approach used to model the material at mesoscopic level as well as the constitutive models applied to describe the dissipative phenomena which occur during the loading process. Therefore, this section is divided into two sections: first one presents the homogenization-based approach applied on the mesoscopic level; constitutive models (cohesive law and plasticity), where the constitutive models used on the numerical simulations are briefly described.

The proposed formulation represents the mechanical behavior of a particular point of the macro-continuum that can be an integration point of a finite element. By solving the macrostructure problem, this point is subjected to a strain tensor that is imposed to the microstructure and, then the stress and constitutive tensors related to that point of the macro-continuum can be computed after solving the microstructure problem, Pèric *et al.* (2011) and Fernandes *et al.* (2015a). For that, the material microstructure is defined as RVE, whose dimensions are not important, but the distribution and proportionality of the materials which compose the microstructure affect its behavior, Pituba *et al.* (2016), Santos *et al.* (2016), Santos and Pituba (2017). Adopting concepts of volumetric average and energy equivalence between the macro and micro-continuum, different values for the homogenized stress and constitutive tensors can be obtained according to the multi-scale model adopted, which depends on the boundary conditions adopted for the RVE. Note that in this work, the material microstructure is analyzed in the context of multi-scale analysis, where different RVEs subjected to a strain tensor have been analyzed, but a full coupled multi-scale analysis of a structure is not presented.

Therefore, to simulate the concrete mechanical behavior, a RVE is used to represent the material at mesoscopic level, whose discretization by Finite Element Method is shown in Fig. 1. The aggregates are considered approximately circular (Nguyen *et al.* 2010), where elastic triangular finite elements are defined, while the matrix can present elastoplastic behavior governed by the Mohr-Coulomb model. Besides, cohesive-contact finite elements are used to model the interface zone in order to simulate the opening and/or closure of fractures that occur, mainly in this region, leading to dissipative phenomena during the fracture process of the concrete microstructure. It is important to note that the cohesive contact finite elements used in this work

are composed of two surfaces which are coincident in the undeformed configuration of the RVE. The cohesive contact finite element is defined as an element with four nodes and its geometry is compatible with the two triangle finite elements used to model the matrix and aggregate zones. The formulation of the cohesive contact finite element is presented in Pituba and Souza Neto (2015) and Pituba *et al.* (2016).

Note that the proposed model is used to simulate the mechanical behavior of the conventional concretes with compressive strength up to 50 MPa. Besides, the proposed modeling presented can also be used to model high strength concretes, however the dissipative phenomena which occur at the mesoscopic level also includes a quasi-brittle behavior of the aggregates and a more rigid behavior of the matrix due to the improvement of its mechanical properties affected by w/c relation, porosity and others. Therefore, it is necessary to consider possible fractures in the aggregates. Nevertheless, that fracture process with the phase debonding in the ITZ can lead to damage localization at mesoscopic level and a consequent macrocrack nucleation. This kind of problems will be addressed in future works where the present formulation must be improved, see Fernandes *et al.* (2015a), Fernandes *et al.* (2015b) and Toro *et al.* (2016).

2.1 Homogenization-based approach, an overview

The homogenization-based approach is briefly described as follows. More details can be found in Fernandes *et al.* (2015a), Fernandes *et al.* (2015b) and Pituba *et al.* (2016).

The RVE described in Fig. 1 is considered as a continuum medium, therefore the stress concept is valid at mesoscopic level. The macroscopic quantities for strain $c(x,t)$ and stress $\sigma(x,t)$ at a point x of the macro-continuum are defined as the volumetric average of their respective field $\varepsilon_\mu=\varepsilon_\mu(y,t)$ or $\sigma_\mu=\sigma_\mu(y,t)$ over the RVE, considering all points y of the RVE related to the point x. Thus, for an arbitrary instant t the following expressions are defined

$$\boldsymbol{\varepsilon}(x,t)=\frac{1}{V_{\boldsymbol{\mu}}}\int_{\Omega_{\boldsymbol{\mu}}}\boldsymbol{\varepsilon}_{\boldsymbol{\mu}}(y,t)\,dV \tag{1}$$

$$\boldsymbol{\sigma}(x,t)=\frac{1}{V_{\boldsymbol{\mu}}}\int_{\Omega_{\boldsymbol{\mu}}}\boldsymbol{\sigma}_{\boldsymbol{\mu}}(y,t)\,dV \tag{2}$$

Eqs. (1) and (2) represent the macroscopic or homogenized values for strain and stress because the microscopic fields have been transformed into macroscopic quantities by means of a homogenization technique. Besides, the microscopic stress can be written in terms of the microscopic strain, as follows

$$\boldsymbol{\sigma}_{\boldsymbol{\mu}}(y,t)=f_y(\boldsymbol{\varepsilon}_{\boldsymbol{\mu}}(y,t)) \tag{3}$$

where f_y is the constitutive functional, defined in this work by the Mohr-Coulomb model. Moreover, the microscopic strain ε_μ can be written in terms of the microscopic displacement filed $\boldsymbol{u}_\mu$ of the RVE, as follows

$$\boldsymbol{\varepsilon}_{\boldsymbol{\mu}}(y,t)=\nabla^S u_{\boldsymbol{\mu}}(y,t) \tag{4}$$

where ∇^s is the symmetric gradient operator of the displacement field $\boldsymbol{u}$.

Without loss of generality, the microscopic displacement filed $\boldsymbol{u}_\mu$ can be defined as the sum of three parts

$$u_\mu(y,t)=u(x,t)+\bar{u}_\mu(y,t)+\tilde{u}_\mu(y,t) \tag{5}$$

being the first one constant representing a rigid body motion coincident to the macroscopic displacement $\boldsymbol{u}(x,t)$ related to the point x, the second one is obtained from the macroscopic strain $\boldsymbol{\varepsilon}$ as follows

$$\bar{u}_{\boldsymbol{\mu}}(y,t):=\boldsymbol{\varepsilon}(x,t)y \tag{6}$$

which varies linearly with the coordinate y, and a displacement fluctuation field $\tilde{u}_\mu(y,t)$. Thus, Eq. (5) can be written as

$$u_{\boldsymbol{\mu}}(y,t)=\boldsymbol{\varepsilon}(x,t)y+\tilde{u}_{\boldsymbol{\mu}}(y,t) \tag{7}$$

as the macroscopic displacement $u(x,t)$ is a rigid body motion, it has no influence in the stress field at points y of the RVE, therefore it is not taken into account to obtain the solution of the equilibrium problem. Thus, in Eq. (7) $u(x,t)$ has been disregarded, see Giusti *et al.* (2009).

In Eq. (7) the part $\boldsymbol{\varepsilon}y$ varies linearly with y resulting from the multiplication of the macroscopic strain $\boldsymbol{\varepsilon}$ of the RVE, which is constant, by the coordinates of the point y. In the case of having uniform microscopic strain $\boldsymbol{\varepsilon_\mu}$, the displacement fluctuation $\tilde{u}_\mu$ is null. In the RVE the following relations for the microscopic strain $\boldsymbol{\varepsilon_\mu}$ and the microscopic strain fluctuation $\tilde{\boldsymbol{\varepsilon}}_{\boldsymbol{\mu}}$ have to be satisfied

$$\boldsymbol{\varepsilon}_{\boldsymbol{\mu}}=\nabla^S u_{\boldsymbol{\mu}}(y,t) \tag{8}$$

$$\tilde{\boldsymbol{\varepsilon}}_{\boldsymbol{\mu}}=\nabla^S \tilde{u}_{\boldsymbol{\mu}}(y,t) \tag{9}$$

Considering Eqs. (7) to (9) the microscopic strain can also be written as

$$\boldsymbol{\varepsilon}_{\boldsymbol{\mu}}(y,t)=\boldsymbol{\varepsilon}(x,t)+\tilde{\boldsymbol{\varepsilon}}_{\boldsymbol{\mu}}(y,t) \tag{10}$$

After some manipulations (Fernandes *et al.* 2015a), Eq. (10) can be written in terms of velocity, where a microscopic strain velocity is kinematically admissible if

$$\dot{\boldsymbol{\varepsilon}}_{\boldsymbol{\mu}}(y,t)=\nabla^S \dot{u}_{\boldsymbol{\mu}}=\dot{\boldsymbol{\varepsilon}}(x,t)+\dot{\tilde{\boldsymbol{\varepsilon}}}_{\boldsymbol{\mu}}(y,t)\ \forall \dot{\tilde{u}}_{\boldsymbol{\mu}}\in v_{\boldsymbol{\mu}} \tag{11}$$

where v_μ is the space of kinematically admissible displacements of the RVE. More details can be found in Fernandes *et al.* (2015a).

In order to solve the RVE equilibrium problem boundary, conditions in terms of displacement fluctuations must be imposed to the RVE. Then, the numerical response can vary according to the boundary condition adopted.

To simplify the presentation, the inclusion Ω^i_μ and the matrix Ω^m_μ domains will be considered together as the solid domain Ω^S_μ. Neglecting the inertia forces and that the RVE is subjected to the body force $b=b(y,t)$ and to surface force field $t^e=t^e(y,t)$ acting along the boundary, the Principle of Virtual Displacements establishes that the RVE is in equilibrium if, and only if, the stress field $\boldsymbol{\sigma_\mu}$ over Ω_μ satisfies the classic variational equation of the elasticity

$$\int_{\Omega_\mu^S} \sigma_\mu(y,t):\nabla^S \eta dV - \int_{\Omega_\mu^S} b(y,t)\,.\,\eta dV + \int_{\Omega_\mu^v} \sigma_\mu(y,t):\nabla^S \eta dV - \int_{\Omega_\mu^v} b(y,t)\,.\eta dV - \int_{\partial\Omega_\mu} t^e(y,t).\eta dA = 0 \quad \forall \eta \in v_\mu \tag{12}$$

On the other hand, the works of Hill and Mandel (Giusti *et al.* 2009) have established the Macro Homogeneity Principle which defines that the macroscopic stress power in a arbitrary point of the macrocontinuum must be equal to the volumetric average of the microscopic stress power over the RVE related to that point for any movement kinematically admissible of the RVE (Giusti *et al.* 2009). Taking Eq. (11), assuming $\tilde{\hat{u}}_\mu = \eta$ and considering that the voids are in equilibrium, after some manipulations (see details in Fernandes *et al.* 2015a and Fernandes *et al.* 2015b), we can conclude that the Hill-Mandel principle is valid if, and only if, the following integrals are nulls

$$\int_{\partial\Omega_\mu} t^e(y,t).\tilde{\hat{u}}_\mu dA = 0 \qquad \forall\, \tilde{\hat{u}}_\mu \in v_\mu \tag{13}$$

$$\int_{\partial\Omega^S_\mu} b(y,t).\tilde{\hat{u}}_\mu dV = 0 \qquad \forall \tilde{\hat{u}}_\mu \in v_\mu \tag{14}$$

Considering Eqs. (8) and (10) and writing $\boldsymbol{\sigma}_\mu$ as $\boldsymbol{\sigma}_\mu = f_y(\varepsilon_\mu)$, the following Equation in terms of displacement fluctuation can be obtained to represent the equilibrium problem of the solid part of the RVE

$$\int_{\Omega_\mu^S} f_y(\boldsymbol{\varepsilon}(x,t) + \nabla^S \tilde{u}_\mu(y,t)):\nabla^S \boldsymbol{\eta} dV = 0 \qquad \forall \boldsymbol{\eta} \in \boldsymbol{v}_\mu \tag{15}$$

Finally, the formulation is completed by the appropriated choice of the space $\boldsymbol{v}_\mu$, i.e., with the choice of the kinematical restrictions to be imposed to the RVE. Thus, the microscopic equilibrium problem consists of, given the macroscopic strain tensor $\boldsymbol{\varepsilon}$, finding the field $\tilde{u}_\mu \in v_\mu$ such that for each instant t, the Eq. (15) is satisfied. As $\boldsymbol{\eta}$ is an arbitrary field, after the RVE domain discretization into finite elements, whose domain is referred as Ω^h_μ, the following incremental microscopic equilibrium equation must hold for a load increment in time $\Delta t_n = t_{n+1} - t_n$ and a domain discretization h, finding the displacement fluctuation $\tilde{u}_{\boldsymbol{\mu}(n+1)} = \tilde{u}_{\boldsymbol{\mu}(n)} + \Delta\tilde{u}_{\boldsymbol{\mu}(n)}$

$$G_h^{n+1} = \int_{\Omega^h_{\boldsymbol{\mu}}} B^T f_y(\boldsymbol{\varepsilon}_{n+1} + B\tilde{u}_{\boldsymbol{\mu}(n+1)})\, dV = 0 \tag{16}$$

where $\boldsymbol{B}$ is the global matrix relating strain and displacement, Ω^h_μ is the RVE discretized domain. If the load increment is non-linear, Eq. (16) is solved by applying the Newton-Raphson Method which consists of finding the fluctuation correction $\boldsymbol{\delta}\tilde{u}^{i+1}_{\boldsymbol{\mu}}$ for iteration i+1, such that

$$F^i + K^i \boldsymbol{\delta}\tilde{u}^{i+1}_{\boldsymbol{\mu}} = 0 \tag{17}$$

where $\boldsymbol{F}$ is the force vector and $\boldsymbol{K}$ the tangent stiffness matrix of the RVE. After computing the

correction $\delta\tilde{u}_{\mu}^{i+1}$ defined in Eq. (17), the next step is to obtain the displacement fluctuation field to be considered at iteration i+1 given by: $\tilde{u}_{\mu}^{i+1} = \tilde{u}_{\mu}^{i} + \delta\tilde{u}_{\mu}^{i+1}$.

The homogenized stress is computed from Eq. (2), considering that the RVE is composed by voids and a solid part (matrix and aggregates) $\Omega_{\mu} = \Omega_{\mu}^{S} \cup \Omega_{\mu}^{v}$, resulting into

$$\boldsymbol{\sigma} = \boldsymbol{\sigma}(x,t) = \frac{1}{V_{\mu}} \int_{\Omega_{\mu}^{S}} \boldsymbol{\sigma}_{\mu}(y,t)dV + \frac{1}{V_{\mu}} \int_{\Omega_{\mu}^{v}} \boldsymbol{\sigma}_{\mu}(y,t)dV \tag{18}$$

The RVE equilibrium problem is completed with the choice of the kinematical restrictions to be imposed to the RVE, leading to different classes of multi-scale models and consequently to different numerical results (Peric *et al.* 2011). In this work only periodic displacement fluctuations is considered. For that, each RVE side Γ_i^+ whose normal direction is n_i^+, must correspond to an equal side Γ_i^- with normal direction n_i^-, being $n_i^+ = -n_i^-$. Similarly, for each point y^+ defined on Γ_i^+ must exists a point y^- on the side Γ_i^-.To have periodic displacement fluctuation on the boundary of the RVE, for every pair of points (y^+, y^-), the following relation must be verified

$$\tilde{u}_{\mu}(y^+,t) = \tilde{u}_{\mu}(y^-,t) \quad \forall \{y^+, y^-\} \in \partial\Omega_{\mu} \tag{19}$$

2.2 Constitutive models (cohesive law and plasticity)

Pituba and Souza Neto (2015) have proposed an extension of a cohesive fracture law presented in Cirak *et al.* (2005) in order to deal with damage process leading to the complete failure of microstructures in ductile media. In general way, this model has been developed to represent the cracking process where traction is still possible to be transmitted between fracture surfaces. The cohesive free energy is assumed as

$$\phi = \phi(\delta_n, \delta_S, \mathrm{q}) \tag{20}$$

where, δn is the normal opening displacement due to mode *I*; $\boldsymbol{\delta s}$ is the sliding opening displacement due to mode II and $\boldsymbol{q}$ is the internal variable that describes the inelastic processes related to decohesion.

It is possible to assume that the deformation due to sliding opening process is a scalar value independent of the direction of sliding on the cohesive surface, thus $\delta s = |\boldsymbol{\delta s}|$, therefore the behavior has an isotropic characteristic and the cohesive law is written introducing an effective opening displacement expressed by

$$\delta = \sqrt{\beta^2 \delta_S^2 + \delta_n^2} \tag{21}$$

The parameter β assumes different values (from 0 to 1) to the sliding and normal opening displacements given a weight ratio between the sliding and normal directions. On the other hand, the ϕ free energy potential depends of δ, and the cohesive law is expressed as

$$\mathbf{t} = \frac{t}{\delta}(\beta^2 \boldsymbol{\delta}_{\mathbf{S}} + \delta_n \mathbf{n}) \tag{22}$$

where, $\boldsymbol{n}$ is the unit normal to the cohesive surface; $\boldsymbol{\delta s}$ is the sliding opening vector located on the cohesive surface, $\boldsymbol{t}$ is the cohesive traction on the crack; t is a scalar effective traction.

On the other hand, the released cohesive energy in the microstructure of the material proposed in this work (Eq. (20)) is given by

$$\phi = e\sigma_C\delta_C\left[1-e^{\left[-\left(1+\frac{\delta}{\delta_C}\right)\right]}\right] \tag{23}$$

where the law for the scalar effective traction for the loading cases is obtained from Eq. (23)

$$t=\frac{\partial\phi}{\partial\delta}=\sigma_c e^{-\delta/\delta_c} \qquad if\ \ \delta=\delta_{\max}\ and\ \ \dot{\delta}\geq 0 \tag{24}$$

For the scalar effective traction for the unloading cases is proposed a law considering an elastic behavior, i.e., without residual effective opening displacement as follows

$$t=\frac{t_{\max}}{\delta_{\max}}\delta \qquad if\ \ \delta<\delta_{\max}\ or\ \ \dot{\delta}<0 \tag{25}$$

where e is the e-number, σ_c is the maximum tension cohesive normal traction and δc is a characteristic opening displacement that indicates a critical opening. Thus, β, σ_c and δc are parameters of the cohesive model. Besides, $\dot{\delta}$ is the opening displacement rate.

On the other hand, accordingly to Ortiz and Pandolfi (1999), there is a relation between the cohesive law and the critical energy released rate (G_C) for crack propagation in the microstructure. Assuming the direction 1 as the direction on the fracture surface and towards to its propagation, G_C can be written as

$$G_C=\int_0^R t.\delta_{,1}\,dx_1 \tag{26}$$

where R is the cohesive zone length. The Eq. (26) can also be defined as

$$G_C=\int_0^\infty t.\delta_{,1}\,dx_1=\phi_\infty \tag{27}$$

For the cohesive law presented in this work, using Eq. (24), the critical energy released rate is given by

$$G_C=e\sigma_C\delta_C \tag{28}$$

Obviously, the G_C for conventional modeling is developed with phenomenological constitutive models applied on the homogenized macrocontinuum. In the present work, the concept of fracture energy is closely related to that which occurs in the ITZ of the microstructure at mesoscopic level.

Also, in initial loading levels, the cohesive fracture has to be kept closed. Besides, it is necessary to not allow penetration of the surfaces of the fracture when unloading process occurs. Therefore, a strategy based on penalty factor is assumed to create stiffness between the nodes of the embedded cohesive contact finite elements in the matrix zone. This penalty factor effectively

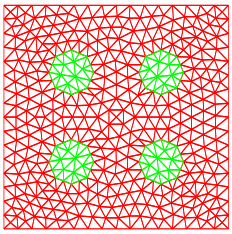

Fig. 2 Representative volume element with 4 inclusions

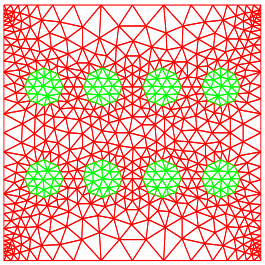

Fig. 3 Representative volume element with 8 inclusions

replaces the initial rigid part of the cohesive law by a linear response given by Eq. (29).

$$t = \lambda_p \delta \qquad if \ \ \lambda_P \delta \leq \sigma_c \tag{29}$$

On the other hand, to deal with plastic strains presented on the macrostructure of the concrete when the material is subjected mainly to compression stress, the well-known Mohr-Coulomb model is used to represent the mechanical behavior of the cement matrix. Therefore, this is another dissipative process to be modeled in the microstructure of the material together the possible microcracking nucleation that occurs mainly in the ITZ. In case of predominant tension regimes, the proposed modeling evidences the microcracking process in the ITZ as the most important dissipative phenomenon, mainly in the initial loading stages. Obviously, the microcracking process in the matrix zone that occurs in the softening regime of the macrostructure of the material is also important leading to insertion of cohesive contact finite elements in the matrix zone. However, these embedded finite elements can generate numerical instabilities, mainly in the peak stress regime. Besides, in predominant compression regimes, the yielding process in the matrix is understood as principal phenomenon in conjunction with the microcracking process in the ITZ.

3. Results and discussions

In order to evaluate the proposed formulation, some numerical analyses applied to quasi-brittle material focusing on mechanical behavior of the concrete microstructure are performed. Initially, RVEs with dimensions $l \times l$ and thickness $l/10$ containing inclusions placed into a matrix are generated. Obviously, the inclusions (aggregates) and matrix have different mechanical properties evidencing the heterogeneous characteristic of the medium submitted to plane stress states. For the matrix zone, an elastopplastic behavior is assumed following the Mohr-Coulomb criterion with the parameter values given by, Assad *et al.* (2014): Young's modulus E is 20 GPa and Poisson ration

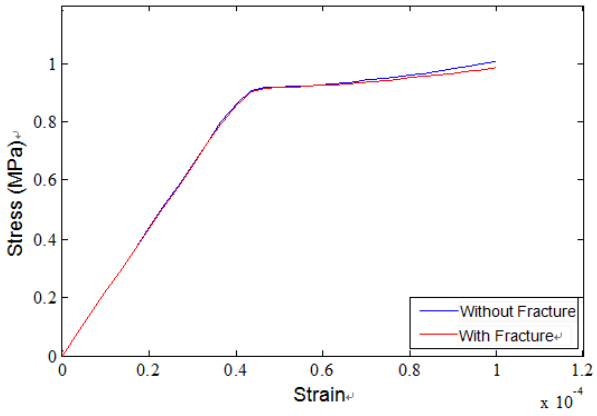

Fig. 4 Homogenized stress in the x-direction versus imposed macroscopic strain on the x-direction for the RVE with 4 inclusions

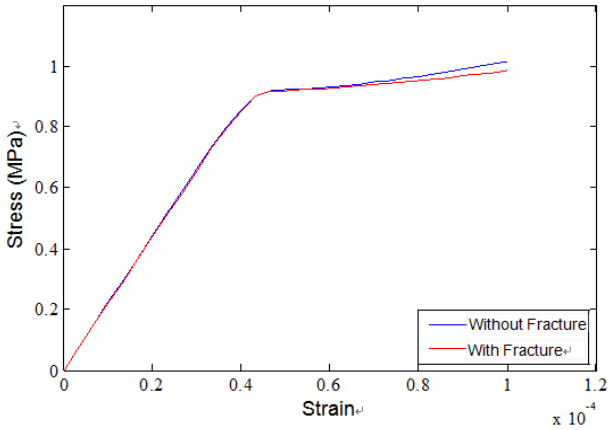

Fig. 5 Homogenized stress in the x-direction versus imposed macroscopic strain on the x-direction for the RVE with 8 inclusions

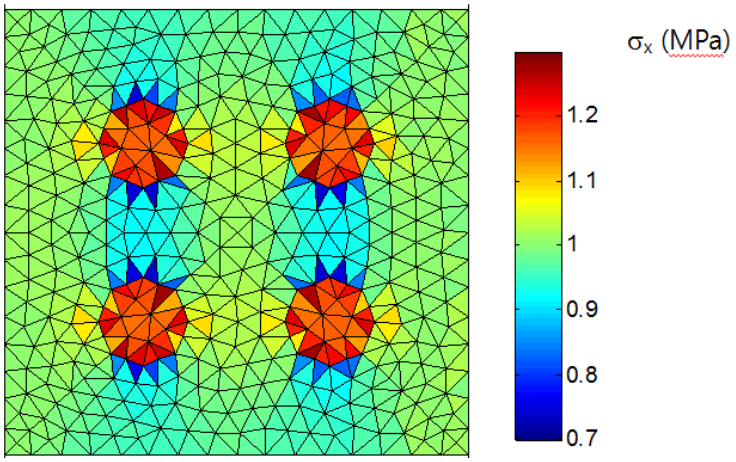

Fig. 6 Stress distribution on the x-direction inside the RVE with 4 inclusions considering perfectly bonded inclusions (aggregates)

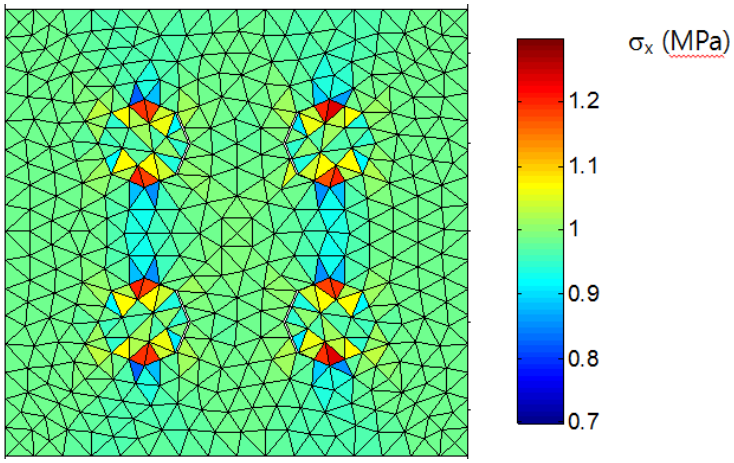

Fig. 7 Stress distribution on the x-direction inside the RVE with 4 inclusions considering phase debonding in the ITZ

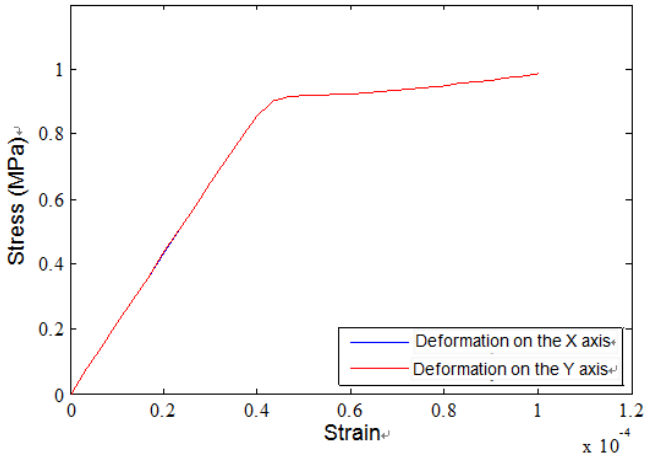

Fig. 8 Homogenized stress on the x-direction versus imposed macroscopic strain for the RVE with 4 inclusions

ν is 0.2, friction angle and dilatation angle are ϕ=5° and Ψ=10%, respectively. The aggregates are considered elastic media with E=35 GPa and ν=0.26, Mehta and Monteiro (2008).

For the ITZ, in the situations where the fracture process has been evaluated, cohesive contact finite elements have been used. The parameters for the cohesive law are given by: λp=200000 N/mm^3, β=0.7, σc=0.09 MPa and δc=0.02 mm, Ortiz and Pandolfi (1999), Oliver *et al.* (2014), Pituba and Souza Neto (2015).

3.1 Influence of the fracture process in the ITZ

In this section, RVEs containing 4 and 8 inclusions with circular shape placed in the matrix zone are analyzed. Fig. 2 presents the RVE with 4 inclusions which represent 12% of volume fraction. For the RVE discretization, 798 triangular finite elements are used as well as 64 cohesive

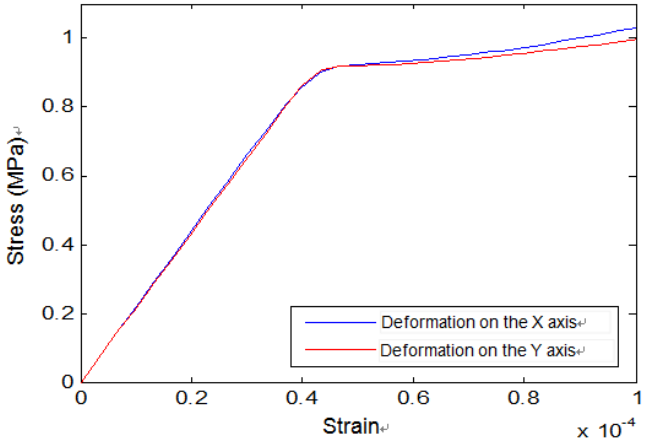

Fig. 9 Homogenized stress on the x-direction versus imposed macroscopic strain for the RVE with 8 inclusions

contact finite elements, when phase debonding is considered in the analyses. Besides, Fig. 3 presents the RVE with 8 inclusions which represent 14% of volume fraction, where 1184 triangular finite elements are used as well as 128 cohesive contact finite elements, when phase debonding is considered in the analyses.

The RVEs have been submitted to a total macroscopic strain ε_x=0,0001 and ε_y=-0,00001 divided in 20 increments. The distortional strain has been considered null. The homogenized stresses versus imposed macroscopic strain for x-direction are plotted in Figs. 4 and 5. Note that the numerical responses considering perfect bonding or fracture process in the ITZ are the same in each RVE for initial loading levels presenting an elastic response. Nevertheless, when the microcrack nucleation in the ITZ is evidenced, the numerical responses present different values. The consideration of fracture process in the ITZ shows an important contribution in the non-linear behavior of the material at mesoscopic level. This conclusion is in agreement with others authors (Metha and Monteiro 2008, Nguyen *et al.* 2010 and Kim and Al-Rub 2011). The cohesive fracture model decreases the stiffness of the RVE beyond the yielding limit which occur in the matrix.

In order to visualize the stress distribution on the x-direction over the RVE, Figs. 7 and 8 illustrate the impact on the numerical response when fracture process in the ITZ is considered. Fig. 6 shows the stress distribution for the RVE containing 4 inclusions considering perfect bonding between inclusions and matrix whereas Fig. 7 represents the RVE considering the fracture process in the ITZ. Note in Fig. 6 that the stresses are perfectly transmitted to rigid inclusions which are responsible for strength of the RVE evidenced by the high stress levels in the inclusions. Therefore, when perfectly bonded inclusions (aggregates) are considered, the homogenized stiffness is higher than the RVE with phase debonding, please see Fig. 4 in the final loading levels. This phenomenon is more evident on the RVE with 8 inclusions due to the more extensive ITZ.

On the other hand, the stress values in the aggregates presented in Fig. 7 are smaller when compared to the Fig. 6 due to the consideration of phase debonding represented by the insertion of the cohesive contact finite elements. Thus, the impact of the aggregates on the homogenized stiffness of the material is smaller, as shown in Figs. 4 and 5.

Therefore, the modeling of the microcracking process in the ITZ is fundamental to estimate the collapse of the concrete microstructure, mainly in predominant tension regimes. This assertion is

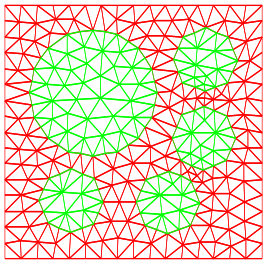

Fig. 10 RVE proposed by Nguyen *et al.* (2010)

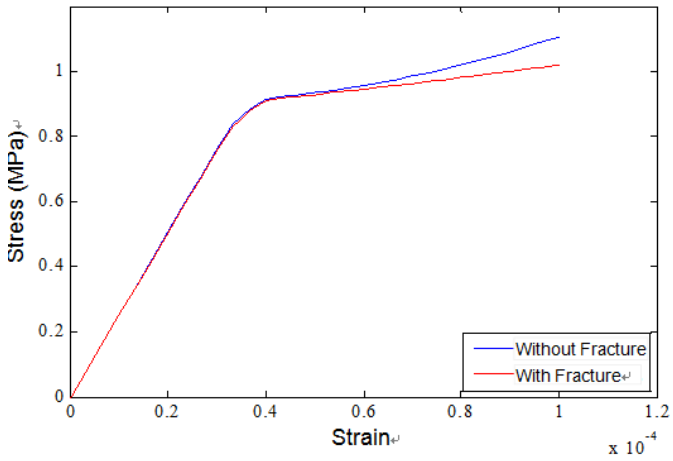

Fig. 11 Homogenized stress on the x-direction versus imposed macroscopic strain on the x-direction for predominant tension regime

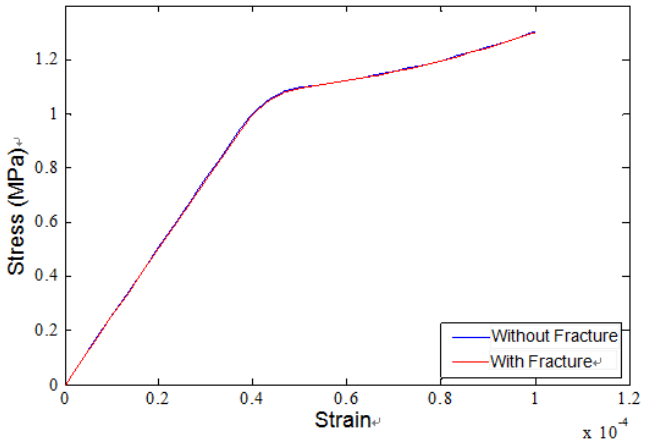

Fig. 12 Homogenized stress (compression) on the x-direction versus imposed macroscopic strain (shortening) on the x-direction for predominant compression regime

based on results obtained by Pituba and Souza Neto (2015) and Kim and Al-Rub (2011). For Pituba and Souza Neto (2015), even considering elastic behavior for the matrix and aggregates, the fracture process in the ITZ modeled by cohesive contact finite elements together with the

geometry of the aggregates allows the simulation of homogenized plastic macroscopic strains in unloading and reversal loadings situations, leading to the capture of the unilateral effect behavior of the concrete.

3.2 Anisotropic behavior

In order to check if the proposed modeling is capable to obtain complex responses on the macrostructure, but as a consequence of which happens in the microstructure, for example, the anisotropic behavior of the concrete is investigate. For this reason, a set of analyses has been performed using the RVEs described in Figs. 2 and 3. Initially, the macro strains ε_x=0.0001 and ε_y=-0.00001 have been imposed. Soon after, ε_y=0.0001 and ε_x=-0.00001 have been applied. The numerical results are presented in Figs. 8 and 9 and they have been expressed by homogenized stress versus imposed macroscopic strains. In Fig. 8 is presented the numerical results for RVE with 4 inclusions whereas Fig. 9 presents the numerical results for RVE with 8 inclusions.

Fig. 8 shows that the mechanical behavior in different directions has been the same. This due to the RVE has symmetry related to the axes *x* and *y*. But in Fig. 9, the mechanical behaviors in different directions present evident differences when the fracture nucleation in the ITZ takes place. In this last case, the non-symmetric distribution of the inclusions in the RVE is responsible for this phenomenon. Therefore, the proposed modeling is capable to capture the anisotropy of the material, a macro-continuum phenomenon, by means the consideration of the inclusion geometries and phase debonding in the ITZ using simple constitutive models at mesoscale level.

3.3 Homogenized responses in tension and compression regimes

In this section, the fracture process in the ITZ for RVEs in predominant tension and compression regimes is evaluated. The RVE proposed by Nguyen *et al.* (2010) is used, see Fig. 10. The first analysis consists in the application of the macroscopic strain simulating a predominant tension regime given by: ε_x=0.0001 and ε_y=-0.00001, where γ_{xy} is approximately null. After that, a predominant compression regime has been considered with the same magnitude. (ε_x=-0.0001 and ε_y=0.00001). The Figs. 11 and 12 present results of the homogenized stress on x-direction versus imposed macroscopic strain on x-direction. For the visualization proposes, Fig. 12 presents positive signals for compressive homogenized stress and macroscopic strains.

Fig. 11 shows the important contribution of the fracture process in predominant tension regime leading to a decreasing of the homogenized stiffness and strength of the material. Fig. 12 shows that the fracture process is not so important in predominant compression regimes. This assertion is based on the mechanical behavior of the cohesive contact finite elements placed in the ITZ. The traction transmission reducing between the fracture surfaces is evident when the value of the cohesive traction increases, but this is not happen in many cohesive contact finite elements in the RVE submitted to predominant compression regime. Therefore, for the analysis displayed in Fig. 12, many cohesive contact finite elements are submitted to compression loading conditions, where the contact law is activated.

3.4 Influence of the fracture process in the matrix zone

In this numerical application, cohesive contact finite elements have been inserted in the matrix zone in order to evaluate the influence of the fracture process on the macroscopic behavior of the concrete. Note that the fracture nucleation in the ITZ is taking into account. The RVE proposed by

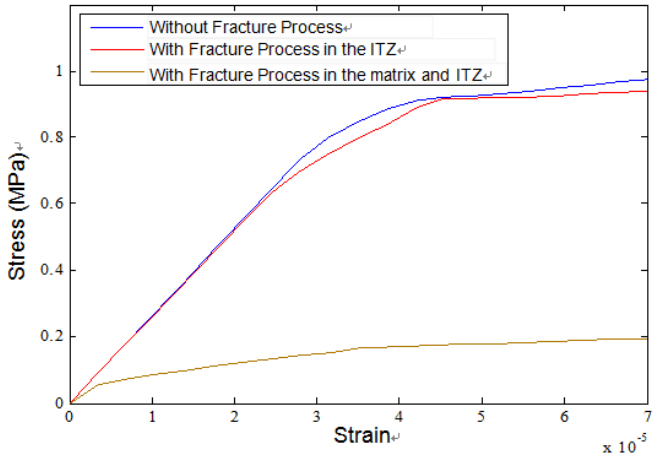

Fig. 14 Homogenized stress on the x-direction versus imposed macroscopic strain on the x-direction for predominant tension regime

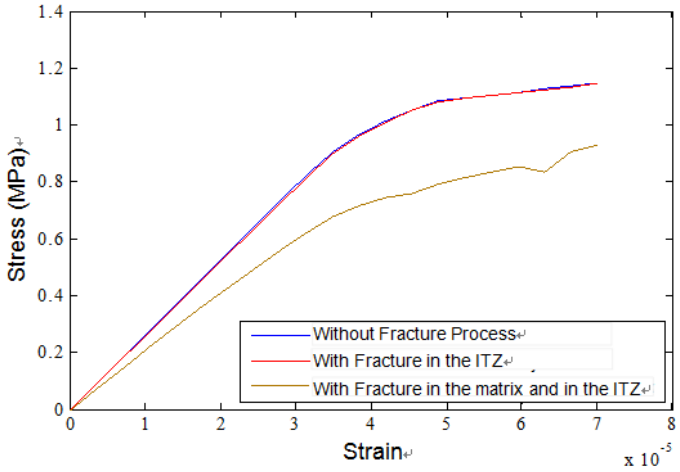

Fig. 15 Homogenized stress (compression) on the x-direction versus imposed macroscopic strain (shortening) on the x-direction for predominant compression regime

Oliver *et al.* (2014) is used (see Fig. 13), where the cracking path is assumed known. The aggregate volume fraction is 22.5% and 3002 triangular finite elements are used. Besides, 120 and 139 cohesive contact finite elements are used in the ITZ and in the matrix zone, respectively.

Three kind of numerical analysis have been performed: the fracture processes are not considered in the matrix and interface transition zones; the second analysis has consisted in the insertion of cohesive fracture finite elements in the ITZ; finally, in the third analysis, the cohesive contact finite elements are inserted in a path in the matrix zone following Oliver *et al.* (2014) as well as the fracture process in the ITZ is considered. For the aggregates, Young's modulus E=100 GPa and Poisson's ratio v=0,2 have been assumed. For the matrix, the parameters for the cohesive law and Mohr-Coulomb model are the same used in previous sections, however for the Young's modulus E=20 GPa and Poisson's ratio v=0,2 have been adopted. The first analysis consists in the application of the macroscopic strain simulating a predominant tension regime given by:

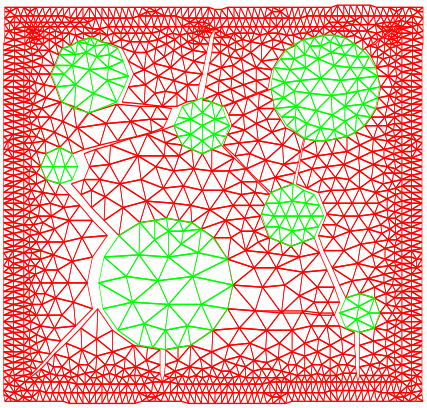

Fig. 16 Finite element mesh in failure regime for the RVE proposed by Oliver *et al.* (2014)

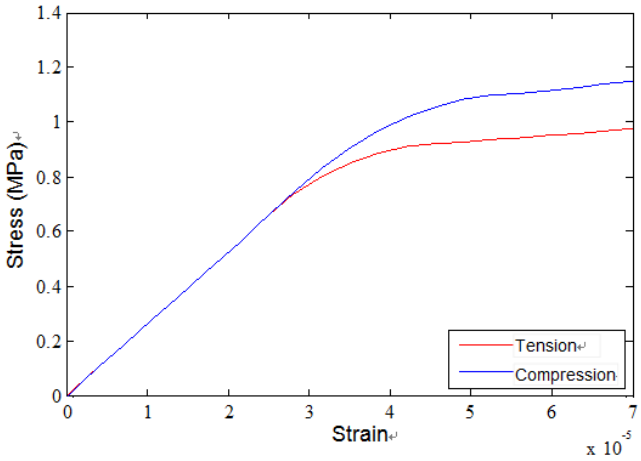

Fig. 17 Homogenized stress on the x-direction versus imposed macroscopic strain on the x-direction for the RVE proposed by Oliver *et al.* (2014)-compression and tension predominant regimes without fracture process

ε_x=0.00007 and ε_y=-0.000007, where γ_{xy} is approximately null. After that, a predominant compression regime has been considered with the same magnitude (ε_x=-0.00007 and ε_y=0.000007). The Figs. 14 and 15 present results of the homogenized stress on x-direction versus imposed macroscopic strain on x-direction. For the visualization proposes, Fig. 15 presents positive signals for compressive homogenized stress and macroscopic strains.

In Fig. 14 is possible to note that the homogenized responses considering or not fracture process in ITZ have presented the expected behaviors accordingly with section 3.1. However, when the fracture process in the matrix zone is considered the RVE has presented a massive strength reduction evidencing an important contribution of the fracture process into the matrix to simulate the failure of the material. The finite element mesh in failure regime of the RVE is shown in Fig. 16.

On the other hand, for predominant compression regime, Fig. 15 shows that there is no difference between the homogenized responses when the fracture process in the ITZ is considered or not. However, when fracture process in the matrix zone is considered the stiffness and strength

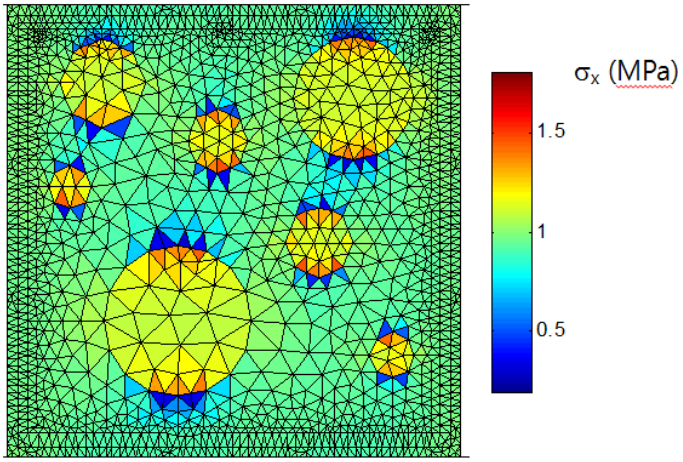

Fig. 18 Stress (MPa) on the x-direction distribution over the RVE for tension predominant regime considering perfect bonding between aggregates and mortar

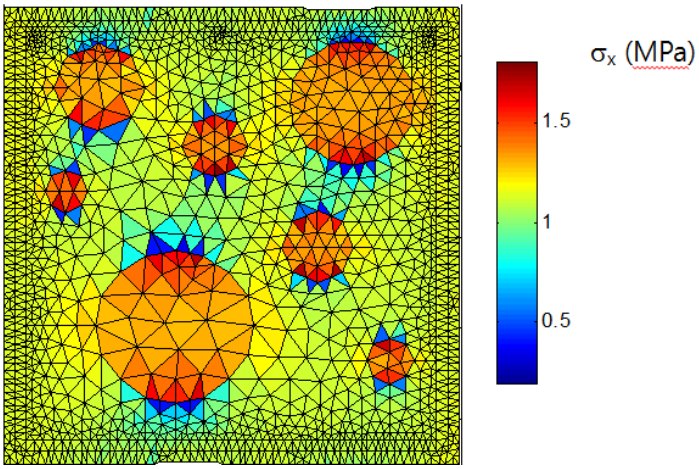

Fig. 19 Stress (MPa) on the x-direction distribution over the RVE for compression predominant regime considering perfect bonding between aggregates and mortar

of the RVE are decreased, but this decreasing is not so evident as in the predominant tension regime (Fig. 14).

The numerical analysis of the RVE considering no fracture process in the ITZ and matrix zones is shown in Fig. 17. Note that the RVE presents high values of stiffness in compression predominant regime than in the tension predominant regime due to the Mohr-Coulomb model applied in the matrix zone. Observe in Fig. 17 that the homogenized stress and macroscopic strains are plotted in absolute values for better visualization.

Despite of capturing a difference between the homogenized responses in tension and compression predominant regimes, the computational homogenized-based approach cannot represent this difference correctly. The fracture process in the ITZ represented by cohesive contact finite elements inserted around the aggregates is fundamental for capturing different numerical responses in tension and compression predominant regimes. If perfect bonding is assumed, i.e., no

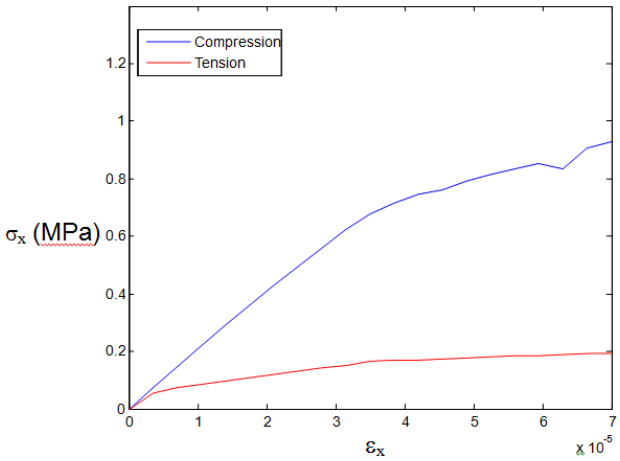

Fig. 20 Homogenized stress on the x-direction versus imposed macroscopic strain on the x-direction for the RVE proposed by Oliver *et al.* (2014)-compression and tension predominant regimes considering fracture process

fracture process is assumed in the ITZ, Fig. 18 shows that a perfect transmission of stresses between the aggregates and mortar is present. This phenomenon leads to an evident increasing of stiffness and strength of the RVE due to the rigid aggregates. Fig. 19 shows the same phenomenon for compression predominant stress, but the stress level has the same magnitude of the tension predominant regimes.

In conclusion, the ITZ has an important role in the dissipative phenomena in microstructures of brittle materials, like concrete. Besides, the consideration of the fracture process in the matrix zone is also important when the failure stage is the focus of the numerical simulation. This assert is evidenced in Fig. 20 where cohesive contact finite elements are inserted in the ITZ and matrix zones. Observe in Fig. 20 that the stress and strains are plotted in absolute values for better visualization.

4. Conclusions

In this work a computational homogenization-based approach has been applied to capture the major characteristics of the mechanical behavior of quasi-brittle materials like concrete. In this context, a computational modeling has been proposed, being the numerical analyses restricted to the mesoscopic level. Using simple constitutive models and defining accordingly the geometry of the different phases of the RVE, some important macroscopic phenomena have been represented.

When cohesive contact finite elements are considered at the ITZ, the deacreasing of stiffness in the homogenized response could be evidenced without presenting total loss of the stress propagation, as expected. Moreover, the incorporation of the plasticity model in the improved multi-scale modeling proved to be satisfactory to overcome the problems presented in Pituba and Souza Neto (2015) when dealing with rigid responses in predominant compression regimes. However, if only plasticity process is considered without fracture process in the ITZ, the numerical results are not satisfactory due to the elastic behavior of the aggregates leading to a not realistic homogenized elastic behavior for the material. Therefore, this work has shown the importance of

considering the dissipative phenomena at ITZ for better representation of the mechanical behavior in quasi-brittle materials.

On the other hand, a limitation of the proposed model in reproducing the softening behavior for predominant tension regimes when occurs the microcracking process inside the mortar has been presented. Besides, the definition of cohesive-contact elements in the matrix can lead to instabilities of the numerical response for predominant tension regimes. To overcome these difficulties, in future works the cohesive-contact finite elements could be replaced for the high aspect ratio elements developed by Rodrigues *et al.* (2016). But for concrete structures, in service regimes, the proposed model has shown to be a proper tool to perform multi-scale analysis of structures.

Although the proposed model presents some limitations, in the numerical examples analyzed in this work, the proposed modeling has captured complex phenomena by adopting simple constitutive models, what encourage us to proceed with this research. The proposed model will be considered for identification of quantitative responses for the concrete, as well as for full coupled multi-scale analyses of concrete structures, based on the works developed in Fernandes *et al.* (2015a) and Fernandes *et al.* (2015b). Moreover, it is important the development of a formulation considering the damage localization phenomenon at microstructure which can lead to a fracture nucleation at macrostructure, as discussed in Sanchéz *et al.* (2013) and Toro *et al.* (2016).

Acknowledgments

The authors wish to thank CAPES Foundation (Ministry of Education of Brazil) and CNPq (National Council for Scientific and Technological Development).

References

Assaad, J.J., Harb, J. and Maaluf, Y. (2014), "Measurement of yield stress of cement pastes using the direct shear test", *J. Non-Newton. Flu. Mech.*, **214**, 18-27.

Brancherie, D. and Ibrahimbegovic, A. (2009), "Novel anisotrtopic continuum-discrete damage model capable of representing localized failure of massive structures. Part I: Theoretical formulation and numerical implementation", *Eng. Comput.*, **26**(1/2), 100-127.

Cirak, F., Ortiz, M. and Pandolfi, A. (2005), "A cohesive approach to thin-shell fracture and fragmentation", *Comput. Meth. Appl. Mech. Eng.*, **194**(21), 2604-2618.

Fernandes, G.R., Pituba J.J.C. and Souza Neto, E.A. (2015a), "Multi-scale modelling for bending analysis of heteregeneous plates by coupling BEM and FEM", *Eng. Anal. Bound. Elem.*, **51**, 1-13.

Fernandes, G.R., Pituba J.J.C. and Souza Neto, E.A. (2015b), "FEM/BEM formulation for multi-scale analysis of stretched plates", *Eng. Anal. Bound. Elem.*, **54**, 47-59.

Gitman, I.M. (2006), "Representative volumes and multi-scale modeling of quasi-brittle materials", Ph.D. Dissertation, Technische Universiteit Delft, The Netherlands.

Giusti, S.M., Blanco, P.J., Souza Neto, E.A. and Feijóo, R.A. (2009), "An assessment of the gurson yield criterion by a computational multi-scale approach", *Eng. Comput.*, **26**(3), 281-301.

Kim, S.M., Al-Rub, R.K.A. (2011), "Meso-scale computational modeling of the plastic-damage response of cementitious composites", *Cement Concrete Res.*, **41**(3), 339-358.

López, C.M., Carol, I. and Aguado, A. (2008), "Meso-structural study of concrete fracture using interface elements. I: Numerical model and tensile behavior", *Mater. Struct.*, **41**(3), 583-599.

Mehta, P.K. and Monteiro, P.J.M. (2008), *Concreto: Estrutura, Propriedades E Materiais*, 1st Edition, PINI,

São Paulo, Brazil.
Miehe, C. (2003), "Computational micro-to-macro transitions for discretized micro-structures of heterogeneous materials at finite strains based on the minimization of averaged incremental energy", *Comput. Meth. Appl. Mech. Eng.*, **192**(5), 559-591.
Miehe, C. and Koch, A. (2002), "Computational micro-to-macro transitions of discretized microstructures undergoing small strains", *Arch. Appl. Mech.*, **72**(4), 300-317.
Needleman, A. and Tvergaard, V. (1987), "An analysis of ductile rupture modes at a crack tip", *J. Mech. Phys. Sol.*, **35**(2), 151-183.
Nguyen, V.P., Lloberas Valls, O., Stroeven, M. and Sluys, L.J. (2010), "On the existence of representative volumes for softening quasi-brittle materials-a failure zone averaging scheme", *Comput. Meth. Appl. Mech. Eng.*, **199**(45), 3026-3036.
Oliver, J., Caicedo, M., Roubin, E., Hernadéz, J.A. and Huespe, A. (2014), *Multi-Scale (FE²) Analysis of Materials Failure in Cement/Aggregate-Type Composite Structure*, In: EURO-C, 2004, St. Anton am Alberg, XX. Anais. Computational Modelling of Concrete Structure, Londres: CRC PRESS, **1**, 39-49.
Ortiz, M. and Pandolfi, A. (1999), "Finite-deformation irreversible cohesive elements for three-dimensional crack-propagation analysis", *J. Numer. Meth. Eng.*, **44**, 1267-1282.
Pereira Jr, W.M., Araújo, D.L. and Pituba, J.J.C. (2016), "Numerical analysis of steel-fiber-reinforced concrete beams using damage mechanics", *Ibrac. Struct. Mater. J.*, **9**(2), 153-191.
Peric, D., Souza Neto, E.A., Feijóo, R.A., Partovi, M. and Carneiro Molina, A.J. (2011), "On micro-to-macro transitions for multiscale analysis of heterogeneous materials: Unified variational basis and finite element implementation", *J. Numer. Meth. Eng.*, **87**(1-5), 149-170.
Pituba, J.J.C. (2015), "A damage model formulation: Unilateral effect and RC structures analysis", *Comput. Concrete*, **15**(5), 709-733.
Pituba, J.J.C. and Fernandes, G.R. (2011), "An anisotropic damage for the concrete", *J. Eng. Mech.*, **137**, 610-624.
Pituba, J.J.C. and Souza Neto, E.A. (2015), "Modeling of unilateral effect in brittle materials by a mesoscopic scale approach", *Comput. Concrete*, **15**(5), 1-25.
Pituba, J.J.C., Fernandes, G.R. and Souza Neto, E.A. (2016), "Modelling of cohesive fracture and plasticity processes in composite microstructures", *J. Eng. Mech.*, **142**(10), 04016069-1-04016069-15.
Rodrigues, E.A., Manzoli, O.L., Bitencourt Jr, L.A.G. and Bittencourt, T.N. (2016), "2D mesoscale model for concrete based on the use of interface element with a high aspect ratio", *J. Sol. Struct.*, **94-95**, 112-124.
Sánchez, P.J., Blanco, P.J., Huespe, A.E. and Feijóo, R.A. (2013), "Failure-oriented multi-scale variational formulation: Micro-structures with nucleation and evolution of softening bands", *Comput. Meth. Appl. Mech. Eng.*, **257**, 221-247.
Santos, W.F. and Pituba, J.J.C. (2017), "Yield surfaces of material composed of porous and heterogeneous microstructures considering phase debonding", *Lat. Am. J. Sol. Struct.*, **14**(7), 1387-1415.
Santos, W.F., Fernandes, G.R. and Pituba, J.J.C. (2016), "Analysis of the influence of plasticity and fracture processes on the mechanical behavior of metal matrix composites microstructures", *Matéria*, **21**(3), 577-598.
Toro, S., Sanchez, P.J. Blanco, P.J., Souza Neto, E.A., Huespe, A.E. and Feijóo, R.A. (2016), "Multiscale formulation for material failure accounting for cohesive cracks at the macro and micro scales", *J. Plast.*, **76**, 75-110.
Wriggers, P. and Moftah, S.O. (2006), "Mesoscale models for concrete: homogenization and damage behavior", *Fin. Elem. Anal. Des.*, **42**(7), 623-636.
Zhu, Q., Kondo, D., Shao, J. and Pensee, V. (2008), "Micromechanical modelling of anisotropic damage in brittle rocks and application", *J. Rock Mech. Min.*, **45**(4), 467-477.